UC Berkeley
UC Berkeley Previously Published Works

Title

Aromaticity and degree of aromatic condensation of char

Permalink

Authors

Wiedemeier, Daniel B
Abiven, Samuel
Hockaday, William C
et al.

Publication Date

2015

DOI

Peer reviewed

Aromaticity and degree of aromatic condensation of char

Daniel B.Wiedemeier[a], Samuel Abiven[a], William C.Hockaday[b], MarcoKeiluweit[c], MarkusKleber[c,d], Caroline A.Masiello[e], Anna V.McBeath[f], Peter S.Nico[g], Lacey A.Pyle[e], Maximilian P.W.Schneider[a], Ronald J.Smernik[f], Guido L.B.Wiesenberg[a], Michael W.I.Schmidt[a]

[a] Department of Geography, University of Zurich, 8057 Zurich, Switzerland
[b] Department of Geology, Baylor University, Waco, TX 76798, USA
[c] Department of Crop and Soil Science, Oregon State University, Corvallis, OR 97331, USA
[d] Institute of Soil Landscape Research, Leibniz Centre for Agricultural Landscape Research (ZALF), 15374 Müncheberg, Germany
[e] Department of Earth Science, Rice University, Houston, TX 77005, USA
[f] School of Agriculture, Food and Wine, University of Adelaide, Adelaide, SA 5064, Australia
[g] Earth Sciences Division, Lawrence Berkeley National Laboratory, Berkeley, CA 94720, USA

Highlights

- Measurements from 38 laboratory chars using 7 characterization methods were compared.

- Most measurements captured the aromaticity or aromatic condensation degree.

- Aromaticity and condensation degree showed distinct patterns with charring temperature.

- Simple methods potentially capture char aromatic features as well as more costly ones.

Abstract

The aromatic carbon structure is a defining property of chars and is often expressed with the help of two concepts: (i) aromaticity and (ii) degree of aromatic condensation. The varying extent of these two features is assumed to largely determine the relatively high persistence of charred material in the environment and is thus of interest for, e.g., biochar characterization or carbon cycle studies. Consequently, a variety of methods has been used to assess the aromatic structure of chars, which has led to interesting insights but has complicated the comparison of data acquired with different methods. We therefore used a suite of seven methods (elemental analysis, MIR spectroscopy, NEXAFS spectroscopy, ^{13}C NMR spectroscopy, BPCA analysis, lipid analysis and helium pycnometry) and compared 13 measurements from them using a diverse sample set of 38 laboratory chars. Our results demonstrate that most of the measurements could be categorized either into those which assess aromaticity or those which assess the degree of aromatic condensation. A variety of measurements, including relatively inexpensive and simple ones, reproducibly captured

the two aromatic features in question, and data from different methods could therefore be compared. Moreover, general patterns between the two aromatic features and the pyrolysis conditions were revealed, supporting reconstruction of the highest heat treatment temperature (HTT) of char.

Graphical abstract
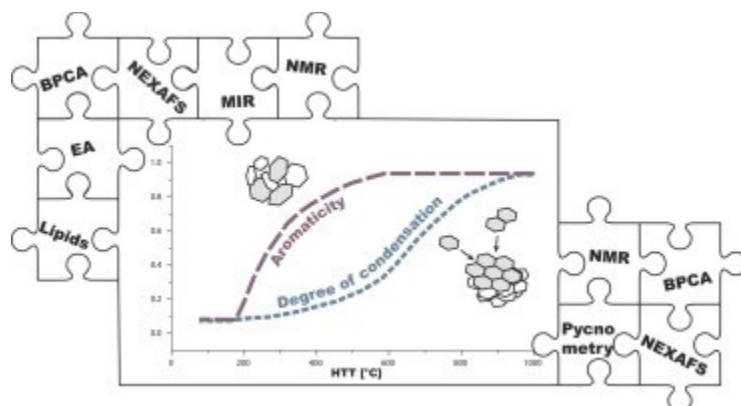
Download high-res image (132KB)

Download full-size image

1. Introduction

Natural and anthropogenic chars have recently received much attention (Manyà, 2012, Knicker, 2011, Glaser and Birk, 2012). Their role as important environmental constituents is increasingly being recognized; chars persist in soils and sediments, which has important implications for the global C budget (Schmidt and Noack, 2000) and they can exert beneficial properties on soils, improving fertility (Biederman and Harpole, 2013) and immobilizing hazardous compounds (Beesley et al., 2011). Moreover, anthropogenic chars (biochars) involve additional economic advantages; prudent biocharproduction can provide green energy, providing an interesting alternative to management of organic waste (Meyer et al., 2011).

With increasing interest in the use of charred material, there is a growing need to characterize and classify the material accurately in order to improve understanding of its properties and behavior in the environment. A defining property of chars and of pyrogenic organic matter in general (Preston and Schmidt, 2006) is their aromatic C structure (Lehmann and Joseph, 2009), which is believed to consist of at least two different aromatic C phases: (i) an amorphous phase comprising randomly organized aromatic rings and (ii) a crystalline phase, comprising condensed

polyaromatic sheets that are turbostratically aligned ([Franklin, 1951](), [Cohen-Ofri et al., 2006](), [Keiluweit et al., 2010]()). The concepts of aromaticity (the total proportion of aromatic C including both phases; [McNaught and Wilkinson, 1997]()) and that of the degree of aromatic condensation (the proportion of the condensed aromatic C only; [McBeath et al., 2011]()) relate to this two phase model. The varying extent of the two phases is believed to largely determine stability of the charred material against degradation in the environment ([Lehmann et al., 2009](), [Singh et al., 2012]()). Consequently, aromaticity and the degree of aromatic condensation of a char likely influence its sequestration potential as well as the duration during which it can provide benefit to the soil ([Nguyen et al., 2010]()).

The two features are themselves influenced by the feedstock, and the [pyrolysis]() conditions. The type of feedstock contributes to the aromaticity and the degree of aromatic condensation by providing different [chemical structures]() as starting material. For example, a high amount of aromatic structures in a feedstock (e.g. [lignin]() in wood) can promote the resulting char aromaticity ([Antal and Grønli, 2003]()). Similarly, different precursor materials attain a high degree of aromatic condensation at different temperatures ([Setton et al., 2002]()). The pyrolysis conditions, in particular the highest [heat treatment]() temperature (HTT), but also residence time, O_2 availability and pressure, influence the C properties of the resulting char ([Shafizadeh, 1982](), [Lua et al., 2004]()). Aromaticity has been reported to increase with HTT from 200 °C to ca. 500 °C, where maximum aromaticity values are reached. The degree of aromatic condensation showed, on the other hand, a more gradual increase with HTT from 400 °C, reaching maximum values at > 1000 °C ([McBeath et al., 2011](), [Schneider et al., 2011]()).

Considering the importance of the aromatic C structure in char and its dependence on many influencing factors, it is not surprising that various attempts have been made to measure these archetypal properties of char. A wide variety of chemical and [physical methods]() has been used, including [elemental analysis](), [molecular markers](), solid state ^{13}C [nuclear magnetic resonance]() (NMR) [spectroscopy](), infrared (IR) spectroscopy, [Raman spectroscopy](), pyrolysis–gas chromatography-mass spectrometry (Py–GC–MS), X-ray diffraction, near edge X-ray absorption fine-structure spectroscopy (NEXAFS), [X-ray photoelectron spectroscopy](), measurement of surface area, He based solid density, electrical resistivity or high resolution [transmission electron microscopy]() (HRTEM) ([Derenne et al., 2005](), [McBeath et al., 2011](), [Charon et al., 2014]()).

While the wealth of methods for aromatic structure characterization of char is fascinating, with the methods continuing to grow in number and quality, it has become increasingly difficult to compare data using different methods and to relate the findings from them. Matters are complicated by the fact that terms such as aromaticity can have multiple technique-specific meanings (McBeath et al., 2011). Moreover, from a practical point of view, researchers and practitioners may have limited resources and instrumentations and would like to optimize both insightful data acquisition and reasonable analysis cost. Efforts to compare different methods and their measurements and to put them in a common framework are therefore required, thereby guiding the interpretation of differently acquired data and suggesting suitable methods for specific analysis problems.

Here, we have used an extensive suite of 7 different methods that provided 13 measurements (cf. Table 1) in a comparative study to evaluate their assessment of the aromatic structure in charred materials. A large sample set, consisting of 38 different laboratory char samples (cf. Table 2), was analyzed using each method. The objective was to show and discuss how the 7 methods and their measurements capture the aromatic structures in the largely different chars and how they compare with each other. Moreover, we aimed to reveal the influence of feedstock, HTT and other pyrolysis parameters on aromaticity and degree of aromatic condensation, by statistically exploring the rich dataset from this large scale comparative study.

Table 1. Methods considered comparatively for assessing aromaticity and/or degree of aromatic condensation of chars (names of derived indices in bold).

Measurement principle	Method	Index (M_{index})	Measurement	Reference
Elemental composition	Elemental analysis	$O–C_{index}$ $H–C_{index}$	C, H and O content (%), H/C, O/C	Baldock and Smernik, 2002, Hammes et al., 2006
Functional groups	Mid-infrared spectroscopy (MIR)	MIR_{index}	Aromaticity ratio (%), $(1420 + 821)/(1510 + 1320)$ cm^{-1}	Wood, 1988, Guo and Bustin, 1998, Moore and Owen, 2001
	Near-edge X-ray absorption fine structure spectroscopy (NEXAFS)	$NEXAFS\text{-}aroma_{index}$ $NEXAFS\text{-}cond_{index}$	Aromaticity ratio (%), 285 eV/286–288 eV Degree of condensation ratio (%), 284 eV/285 eV	Francis and Hitchcock, 1992, Agren et al., 1995, Kuznetsova et al., 2001, Brandes et al., 2008, Keiluweit et

Measurement principle	Method	Index (M_{index})	Measurement	Reference
				al., 2010
	^{13}C Nuclear magnetic resonance spectroscopy (NMR)	**NMR-aroma**$_{index}$	Deconvolution on fitted spectrum with assigned aromatic peaks	McBeath and Smernik (2009), McBeath et al. (2011)
	– with sorbed ^{13}C label	**NMR-cond**$_{index}$	$-\Delta\delta$ (ppm), Shift of sorbed ^{13}C labelled benzene – shift of benzene	
Molecular markers	Benzene polycarboxylic acid (BPCA) analysis	**BPCA-aroma**$_{index}$	Total BPCA amount per organic carbon (g/kg): BPCA/C	Schneider et al. (2011), Wiedemeier et al. (2013)
		BPCA-cond$_{index}$	Ratio of B6CA per total BPCA amount (%), B6CA/BPCA	
	Lipid analysis	**TLE**$_{index}$	Total lipid extract yield (g), TLE	Wiesenberg et al., 2009, Wiesenberg et al., 2010, Wiedemeier et al., 2015
	– n-alkanes	**ACL**$_{index}$	Average chain length, ACL	
	– Polycyclic aromatic hydrocarbons	**PAH**$_{index}$	Ratio of 4–6 ring to 2–3 ring polycyclic aromatic hydrocarbons (%)	
Density	He pycnometry	**Pycno**$_{index}$	Skeletal density (g/cm^3)	Brown et al., 2006, Brewer et al., 2009, Brewer et al., 2014

Table 2. Laboratory chars measured with each method.

Feedstock	Pyrolysis procedure	HTT	n	Thermosequence
Chestnut (Wood) (*Castanea sativa*)	A: 5 h HTT, N$_2$ flow	200–1000 °C	12	Wood-A
Rice (Grass) (*Oryza sativa*)		200–1000 °C	12	Grass-A
Pine (Wood) (*Pinus ponderosa*)	B: 1 h HTT, Closed chamber	100–700 °C	7	Wood-B
Fescue (Grass) (*Festuca arundinacea*)		100–700 °C	7	Grass-B

2. Material and methods

2.1. Char thermosequences

Four different feedstocks (chestnut wood, pine wood, fescue grass and rice grass) and two different pyrolysis procedures (A, 5 h residence time at HTT with continuous N$_2$ flow;

B, 1 h residence time at HTT in a closed chamber) were used to create 38 laboratory char samples with HTT between 100 and 1000 °C (A, 200–1000 °C; B, 100–700 °C), as reported in detail in two previous studies (Keiluweit et al., 2010, Schneider et al., 2011). The resulting char thermosequences (Wood-A, Grass-A, Wood-B, Grass-B) are displayed in Table 2.

2.2. Methods, measurements and derived indices

The char samples were measured using elemental analysis, mid-IR (MIR) spectroscopy, NEXAFS spectroscopy, ^{13}C NMR spectroscopy, benzenepolycarboxylic acid (BPCA) analysis, lipid analysis and He pycnometry, as described in detail in the Supplementary data. Some of the methods provided more than one measurement (e.g. elemental analysis gives H/C ratio and O/C ratio), as summarized in Table 1. Because the measurements are in widely different units and sometimes inversely proportional to each other, indices were built for comparison purposes that project the data on a common scale (0–1) and in the same direction (0, lowest aromaticity or lowest degree of aromatic condensation; 1, highest aromaticity or highest degree of aromatic condensation). Thus, each value x of a measurement M was transformed according to Eq. (1) to provide $M_{index[0-1]}$. In the case of inversely proportional measurements, denoted [1–0], they were further transformed according to Eq. (2) to yield $M_{index[0-1]}$. From here on, the methods and measurements are referred to by their indices (M_{index}), as listed in Table 1.

$$M_{index_{[0-1]} \; or \; [1-0]} = \frac{x_M - min_M}{max_M - min_M} \tag{1}$$

$$M_{index_{[0-1]}} = 1 - M_{index_{[1-0]}} \tag{2}$$

2.3. Data presentation and statistical analysis

The large set of original data can be found in the Supplementary data, while we focus here on the most important findings, showing only simplified data for reasons of clarity and understanding. All data analysis was conducted using the statistical software R (2011). The few missing values (ca. 5%) were imputed with the missForest algorithm (Stekhoven and Buehlmann, 2012) with an estimated normalized root mean square error of only 0.2%. Principal component analysis (PCA; Mardia et al., 1979) including biplots (Gabriel, 1971) was computed on the correlation matrix of the inputed dataset.

3. Results and discussion

All the methods provide measurements of physical or chemical variables linked either to aromaticity or degree of aromatic condensation, but the link between the variables and the derived aromatic features varies greatly. Measuring ring current with NMR (NMR-cond$_{index}$) is, for example, a more direct approach for assessing the degree of aromatic condensation than measuring skeletal density of char with He pycnometry (Pycno$_{index}$). However, the methods differ not only in how they provide assessment of aromatic structures but also in cost, availability and necessary expertise. Moreover, sample amount and composition can prevent the use of one method and/or promote the application of another. For these reasons, the aim was not to identify a reference method via inferential statistics or cost benefit analysis but rather to show method performance and explore qualitatively method similarities and differences within the two categories of aromaticity and aromatic condensation. The standardized measurement results from each method (indices) are shown in full in Fig. 1, Fig. 2 and mathematically summarized according to their resemblance in the form of a PCA, in Fig. 3.
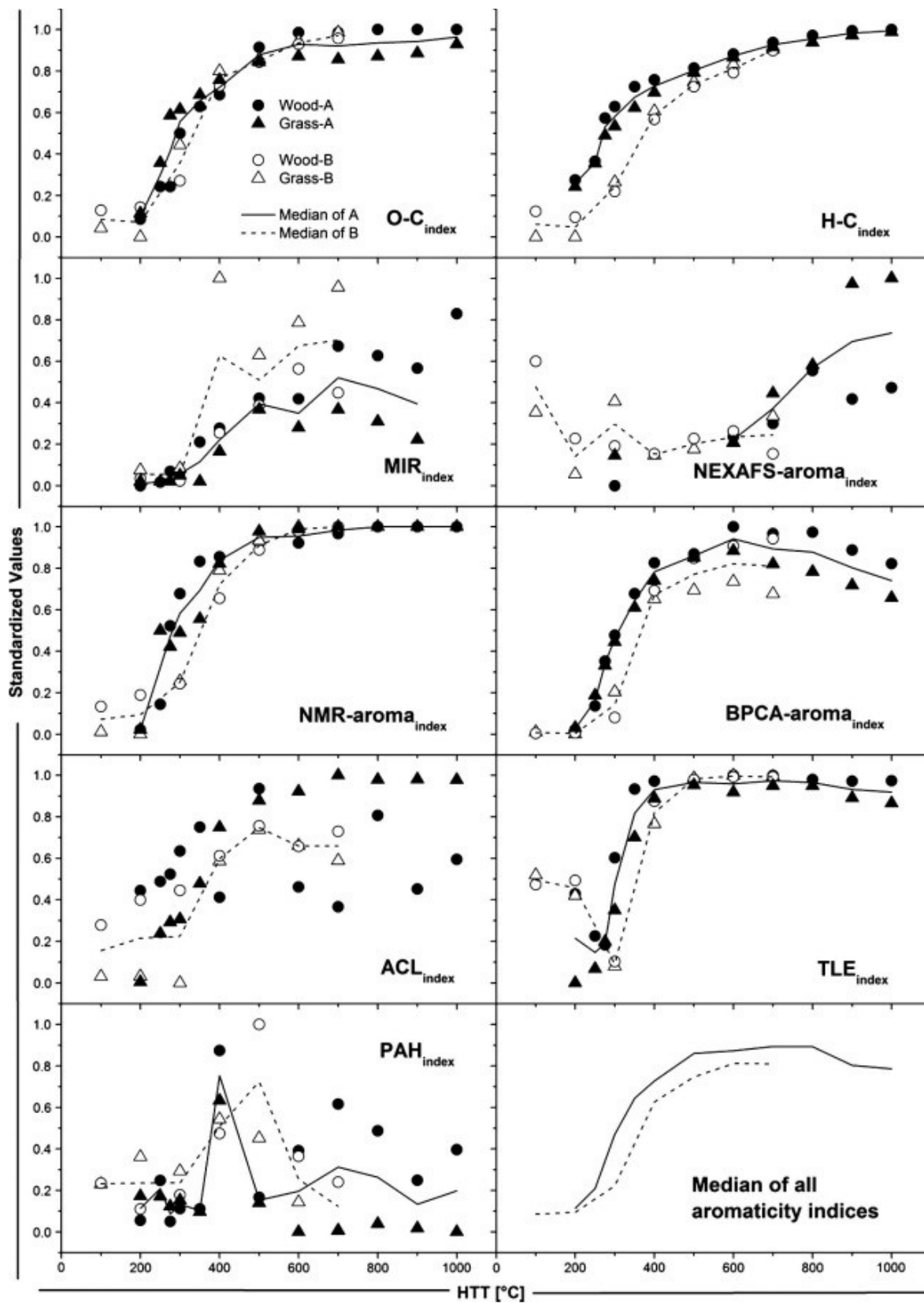
Fig. 1. Char aromaticity as measured via nine different indices. The median of all the indices is shown at the lower right corner and thus describes the typical trend in aromaticity with HTT.
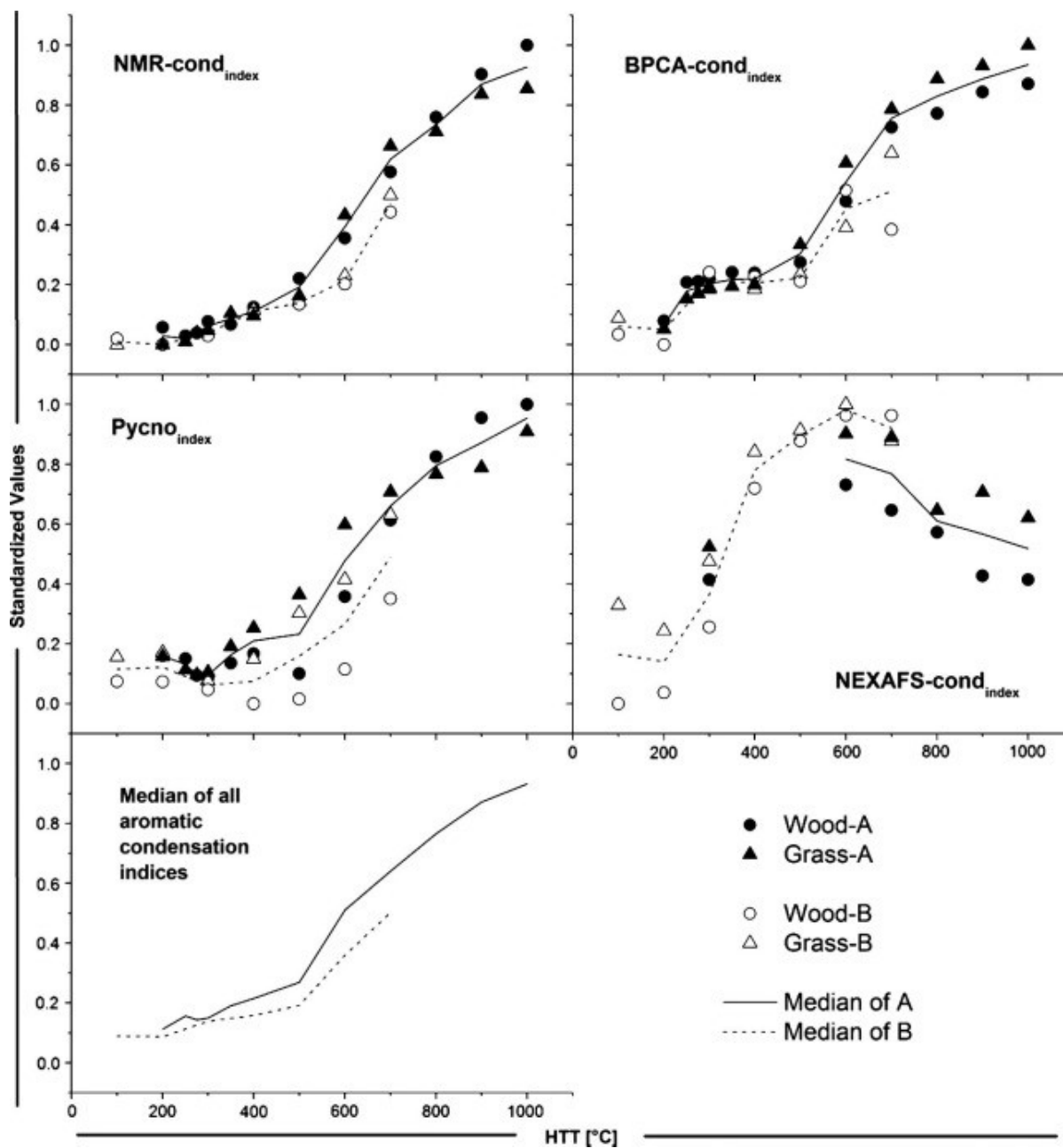
Fig. 2. Degree of aromatic condensation as measured via four different indices. The median of all the aromatic condensation indices is depicted in the lower left and thus shows a typical increase in degree of aromatic condensation with HTT.
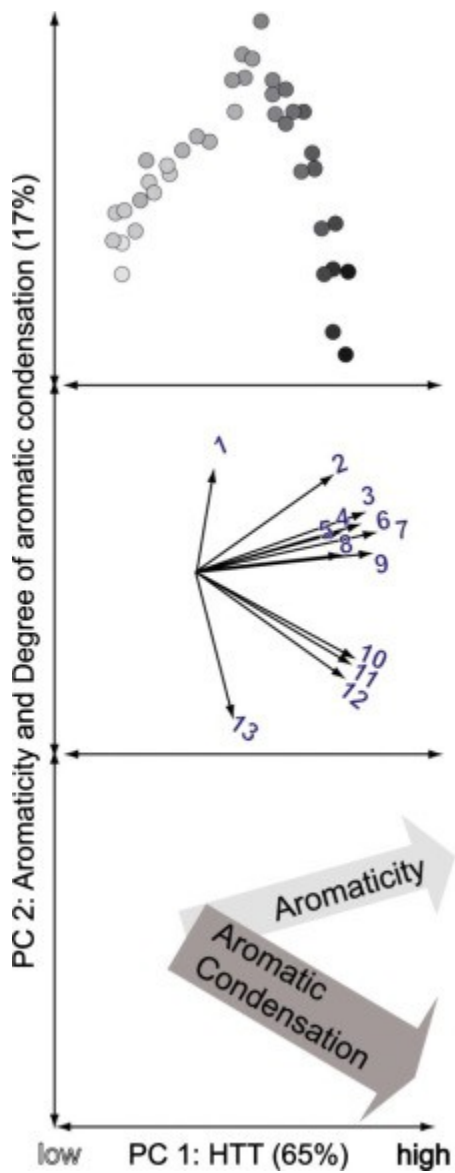
Fig. 3. PCA of the large dataset generated. The first PC is projected along the HTT axis and thus differentiates the chars according to heating temperature. The darker the circle symbol for a sample, the higher its HTT (top). The second PC spreads between aromaticity and the degree of aromatic condensation, showing that the char samples first become more aromatic with increasing HTT and then increase in aromatic condensation in the higher temperatures range (top). Likewise, the PCA differentiates between the different measurements (center and bottom) and groups them into typical aromaticity indices (3–9) and typical indices for assessing the degree of aromatic condensation (10–12). The numbers indicate: 1, PAH_{index}; 2, $NEXAFS\text{-}cond_{index}$; 3, $BPCA\text{-}aroma_{index}$; 4, TLE_{index}; 5, MIR_{index}; 6, $O\text{--}C_{index}$; 7, $NMR\text{-}aroma_{index}$; 8, ACL_{index}; 9, $H\text{--}C_{index}$; 10, $BPCA\text{-}cond_{index}$; 11, $NMR\text{-}cond_{index}$; 12, $Pycno_{index}$; 13, $NEXAFS\text{-}aroma_{index}$.

3.1. Aromaticity

Aromaticity in char is generally easier to assess than the degree of aromatic condensation (McBeath et al., 2011). Thus, more methods are available for measuring aromaticity than for measuring the degree of aromatic condensation (Fig. 1, Fig. 3). In particular, the determination of elemental composition ($O–C_{index}$, $H–C_{index}$), the spectroscopic assessment of functional groups (MIR_{index}, $NEXAFS-aroma_{index}$, NMR-$aroma_{index}$) and the measurement of aromatic molecular markers ($BPCA_{index}$, PAH_{index}) can yield insight into the proportion of aromatic C in chars (Table 1). Non-aromatic molecular markers (TLE_{index}, ACL_{index}) may also be related to the proportion of aromatic C in chars as charring also affects the composition of these moieties.

The $O–C_{index}$ and the $H–C_{index}$ are routine measurements for chars (Baldock and Smernik, 2002, Hammes et al., 2006) and are an indirect measurement of aromaticity because the proportion of C in a sample increases with HTT, as dehydration, depolymerization and volatilization take place, eventually leading to the formation of H and O depleted aromatic C structures (Keiluweit et al., 2010, Wang et al., 2013).

The $O–C_{index}$ of fresh chars depicts a characteristic trend for aromaticity measurements (Fig. 1), because it traces closely the median of all aromatic measurements and thereby shows a typical pattern for aromaticity in the samples: The proportion of aromatic rings in a sample is lowest for low temperature chars, then increases sharply between 200 and 500 °C and reaches a plateau > 600 °C. The increasing $O–C_{index}$ reflects the elimination of O, mostly early in the charring process. The $O–C_{index}$ also differentiates between wood and grass char in the low temperature range (e.g. Wood-B vs. Grass-B). This can be attributed to the higher lignin content of the wood feedstock (Rutherford et al., 2012). At high temperatures, the wood char samples again acquire higher $O–C_{index}$ values than the grass char samples. This probably reflects the higher ash content of the latter, which tends to retard aromatization (Mukome et al., 2013). Despite the fact that O content was assessed differently between the different thermosequences (actual measured O content for the A thermosequences vs. calculated by difference for the B thermosequences – cf. Supplementary data), similar results were obtained in both cases, indicating that the less expensive option of calculating O content by difference may be sufficient for assessing aromaticity in most freshly produced chars. However,

measuring O by difference could be problematic for aromaticity assessment of chars with high ash content.

The H–C$_{index}$ showed the lowest values for aromaticity in the lowest HTT range at 100–200 °C, as expected (Wang et al., 2013). Like the O–C$_{index}$, it also yields higher aromaticity for the lignin-rich wood char samples (Wood-B) than the lignin-poor grass char samples (Grass-B) at these low temperatures. A steep increase in aromaticity then followed from 200–500 °C HTT. However, highest values for H–C$_{index}$ based aromaticity were only reached at the highest HTT (1000 °C), indicating that the H–C$_{index}$ is not a pure measurement for aromaticity. In fact, the H–C$_{index}$ is positioned at the edge of the aromaticity measurements in Fig. 3 (vector number 9), relatively adjacent to the aromatic condensation measurements. This also makes sense from a theoretical point of view, because H is also lost during condensation of aromatic structures at high charring temperature (Franklin, 1951). Thus, the H–C$_{index}$ probably indicates both an increasing amount of aromatic rings, up to ca. 500 °C HTT, and then the increasingly condensed nature of the aromatic rings, that continues to develop at higher charring temperature.

There was a slight lag in aromaticity of the Wood-B and Grass-B thermosequences vs. the Wood-A and Grass-A thermosequences with respect to HTT; the two thermosequences that were charred for 5 h and with a N$_2$ flow (A) attain higher values of aromaticity at slightly lower HTT than the two thermosequences that were charred for only 1 h in closed chambers (B). This pattern was observed for most of the aromaticity measurements (cf. H–C$_{index}$, NMR-aroma$_{index}$, BPCA$_{index}$, TLE$_{index}$) and was independent of feedstock (grass vs. wood). Thus, it appears to be related to the pyrolysismethod, indicating that the longer residence times of pyrolysis procedure A charred the samples more completely at the same HTT than the shorter residence times in procedure B. The slight difference in pyrolysis procedures proved useful in this study because it allowed us to check if the various methods detect this feature.

The MIR$_{index}$ distinguished low temperature chars from high temperature chars, with an increase in aromaticity between 300 and 500 °C, as similarly observed by Harvey et al. (2012a). It can thus serve as a quick and relatively inexpensive screening method for categorizing unknown char samples roughly according to their aromaticity and HTT. However, the MIR$_{index}$ used here only qualifies as a rough estimate for aromaticity, given its large variability for chars > 300 °C, which can also be seen from the shorter length of vector 5 in Fig. 3. Moreover, the MIR$_{index}$ seems to depend on the pyrolysis procedure in

this mid- and high-temperature range, which was not reproduced by any of the other methods. The data show that MIR has the potential to measure aromaticity and possibly other HTT dependent variables, but clearly requires more research and fine tuning with respect to IR bandselection and spectral data analysis.

The NEXAFS-aroma$_{index}$ has been similarly used to describe the B thermosequence chars elsewhere (Keiluweit et al., 2010) and was in the frame of the comparative study now also applied to part of the A thermosequence chars. In the case of the A thermosequence, the NEXAFS-aroma$_{index}$ increased between 600 and 1000 °C. This is unlike most other aromaticity measurements that show a pronounced increase in aromaticity at lower HTT. The NEXAFS-aroma$_{index}$ also gave higher aromaticity values for the Grass-A chars than the Wood-A chars; this is in contrast to most other observations but in line with previous results from NEXAFS applications (Keiluweit et al., 2010). In the case of the B thermosequence, the NEXAFS-aroma$_{index}$ behaved unexpectedly in the low temperature range, indicating high aromaticity values for almost unaltered feedstock and showing decreasing aromaticity with increasing HTT. The reason for the unexpected behavior of the NEXAFS indices is discussed below in Section 3.2.

Using NMR is a recently established means for assessing aromaticity of charred samples (McBeath et al., 2011). The NMR-aroma$_{index}$ determined the wood char samples in the low temperature range (100–200 °C) as being more aromatic than the grass char samples, like the H–C$_{index}$ and O–C$_{index}$, and then also showed the typical increase in aromaticity between 200 and 500 °C, reaching a plateau from 600 °C for all feedstocks and pyrolysis methods, with little variability. Since NMR measures directly the organic C bonds, it is not sensitive to ash content, yielding equally high values for high temperature wood and grass chars. A small shift between the differently pyrolyzed thermosequences (A vs. B) could also be observed where aromaticity increased, further corroborating the idea that the two pyrolysis procedures produced slightly different chars in the mid-temperature range.

The BPCA method separates and quantifies aromatic moieties that originate from condensed aromatic structures, which is why it is insensitive to lignin. Thus, the BPCA-aroma$_{index}$ scored very low for both wood and grass chars in the range up to 200 °C. It then increased steadily with HTT up to 500 °C, where maximum values were reached, and decreased slightly from 700 °C onwards. The trend at low and mid-temperatures was consistent with the other aromaticity measurements, while the slight decrease at

high temperature was inconsistent with the expected high aromaticity at high HTT. This can be attributed to a method artifact from which BPCA-aroma$_{index}$suffers: highly condensed aromatic structures are not completely converted to quantifiable BPCAs and thus, as condensation increases above 600 °C, the BPCA-aroma$_{index}$ declines slightly (Schneider et al., 2010). Still, it is able to distinguish the high temperature chars (grass vs. wood) and also the effect of the two different pyrolysis procedures A and B, which is why the BPCA-aroma$_{index}$ plots well within the aromaticity vector in Fig. 3.

The lipid indices (TLE$_{index}$, ACL$_{index}$, PAH$_{index}$) are indirectly linked to changes in aromaticity because the lipid proportion (e.g. TLE$_{index}$) and quality (e.g. ACL$_{index}$, PAH$_{index}$) vary with HTT and the associated changes in aromaticity. The TLE$_{index}$ showed a typical pattern for the aromaticity measurements, with low values (high extractability) at low temperatures and high values (low extractability) > 600 °C. Simple lipid extraction thus seemed to be a good proxy for aromaticity. It was able to differentiate between the two pyrolysis methods, showing the delayed increase in aromaticity of the B thermosequences, and remained at a constant maximum > 600 °C. However, it suffered from too high index values at low HTT for all thermosequences except the Grass-A thermosequence. This is probably due to the generally low content of extractable lipids in woody tissue (Gocke et al., 2013).

The ACL of alkanes decreases with increasing HTT due to cracking of carbon bonds (Simoneit and Elias, 2000, Wiesenberg et al., 2009), which translates into an increasing trend in the reciprocal ACL$_{index}$ with increasing temperature. The ACL$_{index}$ showed the general pattern of the other aromaticity measurements, e.g. pronounced increase in the index between 200 and 600 °C, a higher lignin-derived aromaticity for woody low temperature chars than grassy chars and the characteristic difference between the two pyrolysis procedures between 200 and 600 °C. However, while the ACL$_{index}$ was similar to other aromaticity measurements for the Grass-A thermosequence, it showed a high variability between the different thermosequences and sometimes no characteristic trend was observable at all (e.g. for the Wood-A thermosequence). These important drawbacks do not seem to depend on pyrolysis method or two types of starting material (wood vs. grass) but rather seem dependent on each of the four individual feedstocks. Thus, using ACL$_{index}$ as an aromaticity measurement requires a careful calibration according to feedstock before conclusions can be drawn from it.

The PAH_{index} is another measurement theoretically linked to aromaticity in chars and which can be retrieved after lipid extraction (Simoneit, 2002, Yunker et al., 2002). Despite its rather straightforward concept of comparing larger with smaller PAH structures, no monotonic trend with HTT was observed. Instead, a maximum of the PAH_{index} was found at 400–500 °C, which interestingly correlates with total solvent-extractable PAH yield, as found in a more detailed study by Keiluweit et al. (2012). These results indicate that the relationship between PAH composition and HTT of chars is rather complex (Wiedemeier et al., 2015) and requires more research.

3.2. Degree of aromatic condensation

We assessed the degree of aromatic condensation by investigating functional groups and atomic bonds (NMR-$cond_{index}$, NEXAFS-$cond_{index}$), quantifying molecular markers (BPCA-$cond_{index}$) and measuring the structural density (Pycno$_{index}$) of the chars (Table 1).

The NMR method is the most recent development in the field and had already afforded plausible results on one set of the chars (Wood-A thermosequence; McBeath et al., 2011). In the same study, it was shown that the degree of aromatic condensation increases more gradually with increasing HTT than aromaticity and that a high degree of condensation only occurs at high HTT. Here, the inclusion of the Grass-A, Wood-B and Grass-B thermosequences again showed a similar pattern: the degree of aromatic condensation was minimal up to 250 °C and then constantly and monotonically increased up to the highest HTT. Interestingly, the chars from the B pyrolysis procedure again lagged behind those from the A pyrolysis procedure, indicating that the shorter pyrolysis time not only reduced the aromaticity but also the degree of aromatic condensation.

The BPCA method reproduced the NMR-$cond_{index}$ general pattern consistently, despite the large difference in methodology. The relationship between the degree of aromatic condensation and HTT was more curved than that for NMR, pointing to a slightly non-linear behavior of the BPCA-$cond_{index}$. This minor deviation is probably method inherent because it occurred reproducibly for all the thermosequences. However, it is surprising that the grass chars scored higher with respect to aromatic condensation than the wood chars at high temperature. This probably reflects the lower BPCA yield from grass chars than wood chars at high temperature (cf. Fig. 1, BPCA-aroma$_{index}$). This effect therefore has to be taken into account when the BPCA-$cond_{index}$ is used for the assessment of the degree of aromatic condensation in chars from different feedstocks.

He pycnometry represents a third, completely independent approach for assessing the degree of aromatic condensation. He can penetrate the smallest of pores and can thus be used to assess the skeletal density (Brewer et al., 2014), which increases with increasing molecular condensation. Despite its lower cost and shorter analysis time, this indirect measurement appeared to reproduce quite well the main trend from the above, more complex and expensive aromatic condensation measurements. It depicted a rather linear increase in aromatic condensation from 300 °C up to the highest measured HTT. He pycnometry measurements in the low temperature range (< 300 °C) seem, however, to be less promising because the $Pycno_{index}$ overestimated aromatic condensation for such mild heat treatment. Besides, the Wood-B thermosequence showed unusual behavior, whereby only the highest HTT (700 °C) would be assigned as giving a condensed aromatic carbon structure.

The $NEXAFS\text{-}cond_{index}$ indicated a pronounced increase in the degree of aromatic condensation of the chars between 200 and 500 °C and a decrease above 600 °C, which is not consistent with the other aromatic condensation measurements (Fig. 3, vector 2). Both NEXAFS indices used here ($NEXAFS\text{-}aroma_{index}$ and $NEXAFS\text{-}cond_{index}$) showed different behavior compared with other metrics of aromaticity and aromatic condensation. The use of simple indices derived from NEXAFS spectra is most likely limited by the fact that resonances in NEXAFS are not derived exclusively from specific functional groups but rather are a result of the entire electronic structure of the char material.

3.3. General patterns of aromatic features and implications

Applying a large suite of 7 methods with 13 measurements to a diverse char sample set of four thermosequences enabled us to identify general patterns between analytical methods and char C properties.

One observable pattern was the distinction between measurements that assess aromaticity and those that assess the degree of aromatic condensation, as discussed above and shown in Fig. 3. The differentiation was sharp and resulted in two distinct trends with HTT as depicted in Fig. 1and Fig. 2. The two general trends across methods are best represented by the median of all measurements for each category: aromaticity increased sharply from 200 °C on, reaching maximum values at 500–600 °C, and stayed constant at the maximum with higher HTT (Fig. 1, bottom right). The median of all aromatic condensation measurements, on the other hand, increased smoothly from

300 °C on, reaching highest values at 1000 °C ([Fig. 2](), bottom left). While this difference between the two categories of aromatic measures has been reported elsewhere ([McBeath et al., 2011]()), it was somewhat surprising how congruently the methods behaved within each category, despite the fact that they are based on fundamentally different approaches. The $O–C_{index}$, for example, followed the $NMR-aroma_{index}$, with only very minor differences for all thermosequences, and the $H–C_{index}$, as well as the $BPCA-aroma_{index}$, gave very similar results. Likewise, $NMR-cond_{index}$, $BPCA-cond_{index}$ and $Pycno_{index}$ were very similar for the degree of aromatic condensation for all feedstocks and pyrolysis procedures. Even the slight shift between pyrolysis procedures A and B with respect to HTT was readily detected with most of the methods ($O–C_{index}$, $H–C_{index}$, $NMR-aroma_{index}$, $BPCA-aroma_{index}$, TLE_{index}, $NMR-cond_{index}$, $BPCA-cond_{index}$, $Pycno_{index}$) reflecting both the importance of the pyrolysis conditions on the char C properties and the high sensitivity of each measurement for differences in char aromatic structure. Our observations imply that a variety of measurements are suitable for assessing the aromatic C structure of chars and that differently acquired data, e.g. from different research groups and laboratories, can be compared if the data are reasonably standardized and calibrated. More comparable [data interpretations]() of diverse published and future studies alike can lead to a more consistent and better understanding of the C structure in different chars, which, in turn, promises to illuminate the C sequestration potential of diverse chars ([Keiluweit et al., 2010](), [Singh et al., 2012](), [Harvey et al., 2012b](), [Wang et al., 2013]()).

The distinctive and reproducibly measurable trends in aromaticity and aromatic condensation as a function of HTT also allow the inverse examination of chars: if the aim is to determine the unknown HTT of a certain char, it can be estimated by measuring its aromatic C structure. A quick multiple linear [regression analysis]() of our dataset (data not shown) indicated that it is best to combine a measurement of aromaticity with one of aromatic condensation to obtain precise HTT reconstruction estimates. Aromaticity and aromatic condensation increase over different ranges of temperature and thus yield complementary information about the char HTT. Methods that provide both aromatic measurements at the same time (e.g. $NMR-aroma_{index}$ and $NMR-cond_{index}$ or $BPCA-aroma_{index}$ and $BPCA-cond_{index}$) are thus beneficial from this point of view. However, similarly good results for HTT reconstruction were achieved by combining different methods, e.g. the $O–C_{index}$, which captures aromaticity, with the $Pycno_{index}$, which measures the degree of aromatic condensation. HTT reconstruction of chars may be an important application of the above methods in archeological studies

([Conedera et al., 2009](#), [Wolf et al., 2013](#)) in addition to the more established focus on char stability in an environmental context ([Nguyen et al., 2010](#), [Al-Wabel et al., 2013](#)).

We conclude that some indirect, relatively inexpensive and simple methods (e.g. [elemental analysis](#) or He pycnometry) captured the aromatic structures in fresh chars similarly well as more costly and time-consuming techniques. This holds promise, whereby aromaticity and the degree of aromatic condensation can be readily assessed in all kinds of char studies and with a variety of new and established methods. Thus, characterization and classification of charred materials should explicitly take these two C aromatic features into account because they are likely key to their stability against degradation in the environment as well as being informative about production temperature.

Author Contributions

D.B.W. compiled and analyzed the data, and wrote the paper. M.W.I.S. conceived and coordinated the comparative study. Samples were provided by M.P.W.S., M. Ke and M. Kl. Analysis was performed by S.A. (MIR), A.V.M., R.J.S. and W.C.H (NMR), M. Ke and P.S.N. (NEXAFS), L.A.P. and C.A.M. (pycnometry), M.P.W.S. and A.V.M. (BPCA), G.L.B.W. (PAH and [lipid](#)analysis). All authors provided input into the drafting and the final version of the manuscript.

Acknowledgments

References

1. **Agren et al., 1995**
   H. Agren, O. Vahtras, V. Carravetta
   Near-edge core photoabsorption in polyacenes – model molecules for graphite
   Chemical Physics, 196 (1995), pp. 47-58

2. **Al-Wabel et al., 2013**

M.I. Al-Wabel, A. Al-Omran, A.H. El-Naggar, M. Nadeem, A.R.A. Usman
Pyrolysis temperature induced changes in characteristics and chemical composition of biochar produced from conocarpus wastes
Bioresource Technology, 131 (2013), pp. 374-379

3. **Antal and Grønli, 2003**
   M.J. Antal, M. Grønli
   The art, science, and technology of charcoal production
   Industrial & Engineering Chemistry Research, 42 (2003), pp. 1619-1640

4. **Baldock and Smernik, 2002**
   J. Baldock, R. Smernik
   Chemical composition and bioavailability of thermally altered Pinus resinosa (Red pine) wood
   Organic Geochemistry, 33 (2002), pp. 1093-1109

5. **Beesley et al., 2011**
   L. Beesley, E. Moreno-Jiménez, J.L. Gomez-Eyles, E. Harris, B.Robinson, T. Sizmur
   A review of biochars' potential role in the remediation, revegetation and restoration of contaminated soils
   Environmental Pollution, 159 (2011), pp. 3269-3282

6. **Biederman and Harpole, 2013**
   L.A. Biederman, W.S. Harpole
   Biochar and its effects on plant productivity and nutrient cycling: a meta-analysis
   GCB Bioenergy, 5 (2013), pp. 202-214

7. **Brandes et al., 2008**
   J. Brandes, G. Cody, D. Rumble, P. Haberstroh, S. Wirick, Y. Gelinas
   Carbon K-edge XANES spectromicroscopy of natural graphite
   Carbon, 46 (2008), pp. 1424-1434

8. **Brewer et al., 2009**
   C. Brewer, K. Schmidt Rohr, J. Satrio, R. Brown
   Characterization of biochar from fast pyrolysis and gasification systems
   Environmental Progress & Sustainable Energy, 28 (2009), pp. 386-396

9. **Brewer et al., 2014**
   C.E. Brewer, V.J. Chuang, C.A. Masiello, H. Gonnermann, X. Gao, B.Dugan, L.E. Driver, P. Panzacchi, K. Zygourakis, C.A. Davies
   New approaches to measuring biochar density and porosity
   Biomass and Bioenergy, 66 (2014), pp. 176-185

10. **Brown et al., 2006**
    R.A. Brown, A.K. Kercher, T.H. Nguyen, D.C. Nagle, W.P. Ball
    Production and characterization of synthetic wood chars for use as surrogates for natural sorbents

Organic Geochemistry, 37 (2006), pp. 321-333

11. **Charon et al., 2014**
E. Charon, J.N. Rouzaud, J. Aléon
Graphitization at low temperatures (600–1200 °C) in the presence of iron implications in planetology
Carbon, 66 (2014), pp. 178-190

12. **Cohen-Ofri et al., 2006**
I. Cohen-Ofri, L. Weiner, E. Boaretto, G. Mintz, S. Weiner
Modern and fossil charcoal: aspects of structure and diagenesis
Journal of Archaeological Science, 33 (2006), pp. 428-439

13. **Conedera et al., 2009**
M. Conedera, W. Tinner, C. Neff, M. Meurer, A.F. Dickens, P. Krebs
Reconstructing past fire regimes: methods, applications, and relevance to fire management and conservation
Quaternary Science Reviews, 28 (2009), pp. 555-576

14. Derenne et al., 2005
S. Derenne, J.N. Rouzaud, C. Clinard, F. Robert
Size discontinuity between interstellar and chondritic aromatic structures: a high-resolution transmission electron microscopy study
Geochimica et Cosmochimica Acta, 69 (2005), pp. 3911-3918

15. **Francis and Hitchcock, 1992**
16. J.T. Francis, A.P. Hitchcock
Inner-shell spectroscopy of a para-benzoquinone, hydroquinone, and phenol – distinguishing quinoid and benzenoid structures
Journal of Physical Chemistry, 96 (1992), pp. 6598-6610

17. **Franklin, 1951**
R.E. Franklin
Crystallite growth in graphitizing and non-graphitizing carbons
Proceedings of the Royal Society, Mathematical, Physical and Engineering Sciences, 209 (1951), pp. 196-218

18. **Gabriel, 1971**
K.R. Gabriel
The biplot graphic display of matrices with application to principal component analysis
Biometrika, 58 (1971), pp. 453-467

19. **Glaser and Birk, 2012**
B. Glaser, J.J. Birk
State of the scientific knowledge on properties and genesis of Anthropogenic Dark Earths in Central Amazonia (terra preta de Índio)
Geochimica et Cosmochimica Acta, 82 (2012), pp. 39-51

20. **Gocke et al., 2013**
M. Gocke, Y. Kuzyakov, G.L.B. Wiesenberg
Differentiation of plant derived organic matter in soil, loess and rhizoliths based on n-alkane molecular proxies
Biogeochemistry, 112 (2013), pp. 23-40

21. **Guo and Bustin, 1998**
Y. Guo, R.M. Bustin
FTIR spectroscopy and reflectance of modern charcoals and fungal decayed woods: implications for studies of inertinite in coals
International Journal of Coal Geology, 37 (1998), pp. 29-53

22. **Hammes et al., 2006**
K. Hammes, R. Smernik, J. Skjemstad, A. Herzog, U. Vogt
Synthesis and characterisation of laboratory-charred grass straw (Oryza saliva) and chestnut wood (Castanea sativa) as reference materials for black carbon quantification
Organic Geochemistry, 37 (2006), pp. 1629-1633

23. **Harvey et al., 2012a**
O.R. Harvey, B.E. Herbert, L.-J. Kuo, P. Louchouarn
Generalized two-dimensional perturbation correlation infrared spectroscopy reveals mechanisms for the development of surface charge and recalcitrance in plant-derived biochars
Environmental Science & Technology, 46 (2012), pp. 10641-10650

24. **Harvey et al., 2012b**
O. Harvey, L.-J. Kuo, A. Zimmerman, P. Louchouarn, J. Amonette, B.Herbert
An index-based approach to assessing recalcitrance and soil carbon sequestration potential of engineered black carbons (biochars)
Environmental Science & Technology, 46 (2012), pp. 1415-1421

25. **Keiluweit et al., 2010**
M. Keiluweit, P.S. Nico, M.G. Johnson, M. Kleber
Dynamic molecular structure of plant biomass-derived black carbon (biochar)
Environmental Science & Technology, 44 (2010), pp. 1247-1253

26. **Keiluweit et al., 2012**
M. Keiluweit, M. Kleber, M.A. Sparrow, B.R.T. Simoneit, F.G. Prahl
Solvent-extractable polycyclic aromatic hydrocarbons in biochar: influence of pyrolysis temperature and feedstock
Environmental Science & Technology, 46 (2012), pp. 9333-9341

27. **Knicker, 2011**
H. Knicker
Pyrogenic organic matter in soil: its origin and occurrence, its chemistry and survival in soil environments

Quaternary International, 243 (2011), pp. 251-263

28. **Kuznetsova et al., 2001**
A. Kuznetsova, I. Popova, J.T. Yates, M.J. Bronikowski, C.B. Huffman, J. Liu, R.E. Smalley, H.H. Hwu, J. G.G. Chen
Oxygen-containing functional groups on single-wall carbon nanotubes: NEXAFS and vibrational spectroscopic studies
Journal of the American Chemical Society, 123 (2001), pp. 10699-10704

29. **Lehmann and Joseph, 2009**
J. Lehmann, S. Joseph
Biochar for environmental management – an introduction
J. Lehmann, S. Joseph (Eds.), Biochar for Environmental Management: Science and Technology, Earthscan, London, UK (2009), pp. 1-12

30. **Lehmann et al., 2009**
J. Lehmann, C. Czimczik, D. Laird, S. Sohi
Stability of biochar in soil
J. Lehmann, S. Joseph (Eds.), Biochar for Environmental Management: Science and Technology, Earthscan, London, UK (2009), pp. 183-206

31. **Lua et al., 2004**
A.C. Lua, T. Yang, J. Guo
Effects of pyrolysis conditions on the properties of activated carbons prepared from pistachio-nut shells
Journal of Analytical and Applied Pyrolysis, 72 (2004), pp. 279-287

32. **Manyà, 2012**
J. Manyà
Pyrolysis for biochar purposes: a review to establish current knowledge gaps and research needs
Environmental Science & Technology, 46 (2012), pp. 7939-7954

33. **Mardia et al., 1979**
K.V. Mardia, J.T. Kent, J.M. Bibby
Multivariate Analysis
Academic Press (1979)

34. **McBeath and Smernik, 2009**
A.V. McBeath, R.J. Smernik
Variation in the degree of aromatic condensation of chars
Organic Geochemistry, 40 (2009), pp. 1161-1168

35. **McBeath et al., 2011**
A. McBeath, R. Smernik, E. Plant
Determination of the aromaticity and the degree of aromatic condensation of a thermosequence of wood charcoal using NMR
Organic Geochemistry, 42 (2011), pp. 1194-1202

36. **McNaught and Wilkinson, 1997**
    A.D. McNaught, A. Wilkinson
    IUPAC. Compendium of Chemical Terminology
    (second ed.), Blackwell Scientific Publications, Oxford (1997)

37. **Meyer et al., 2011**
    S. Meyer, B. Glaser, P. Quicker
    Technical, economical, and climate-related aspects of biochar production technologies: a literature review
    Environmental Science & Technology, 45 (2011), pp. 9473-9483

38. **Moore and Owen, 2001**
    A. Moore, N. Owen
    Infrared spectroscopic studies of solid wood
    Applied Spectroscopy Reviews, 36 (2001), pp. 65-86

39. **Mukome et al., 2013**
    F.N.D. Mukome, X. Zhang, J. Six, S. Parikh, S.J. Parikh
    Use of chemical and physical characteristics to investigate trends in biochar feedstocks
    Journal of Agricultural and Food Chemistry, 61 (2013), pp. 2196-2204

40. **Nguyen et al., 2010**
    B. Nguyen, J. Lehmann, W. Hockaday, S. Joseph, C. MasielloTemperature sensitivity of black carbon decomposition and oxidation
    Environmental Science & Technology, 44 (2010), pp. 3324-3331

41. **Preston and Schmidt, 2006**
    C.M. Preston, M.W.I. Schmidt
    Black (pyrogenic) carbon: a synthesis of current knowledge and uncertainties with special consideration of boreal regions
    Biogeosciences, 3 (2006), pp. 397-420

42. **R, 2011**
    R, 2011.
    R: A Language and Environment for Statistical Computing. R Foundation for Statistical Computing.

43. **Rutherford et al., 2012**
    D.W. Rutherford, R.L. Wershaw, C.E. Rostad, C.N. Kelly
    Effect of formation conditions on biochars: compositional and structural properties of cellulose, lignin, and pine biochars
    Biomass and Bioenergy, 46 (2012), pp. 693-701

44. **Schmidt and Noack, 2000**
    M.W.I. Schmidt, A.G. Noack
    Black carbon in soils and sediments: analysis, distribution, implications, and current challenges
    Global Biogeochemical Cycles, 14 (2000), pp. 777-793

45. **Schneider et al., 2010**
M.P.W. Schneider, M. Hilf, U.F. Vogt, M.W.I. Schmidt
The benzene polycarboxylic acid (BPCA) pattern of wood pyrolyzed between 200 °C and 1000 °C
Organic Geochemistry, 41 (2010), pp. 1082-1088

46. **Schneider et al., 2011**
M.P.W. Schneider, R. Smittenberg, T. Dittmar, M.W.I. Schmidt
Comparison of gas with liquid chromatography for the determination of benzenepolycarboxylic
acids as molecular tracers of black carbon
Organic Geochemistry, 42 (2011), pp. 275-282

47. **Setton et al., 2002**
R. Setton, P. Bernier, S. Lefrant
Carbon Molecules and Materials
CRC Press (2002)

48. **Shafizadeh, 1982**
F. Shafizadeh
Introduction to pyrolysis of biomass
Journal of Analytical and Applied Pyrolysis, 3 (1982), pp. 283-305

49. **Simoneit, 2002**
B.R.T. Simoneit
Biomass burning – a review of organic tracers for smoke from incomplete combustion
Applied Geochemistry, 17 (2002), pp. 129-162

50. **Simoneit and Elias, 2000**
B.R.T. Simoneit, V.O. Elias
Organic tracers from biomass burning in atmospheric particulate matter over the ocean
Marine Chemistry, 69 (2000), pp. 301-312

51. **Singh et al., 2012**
B.P. Singh, A.L. Cowie, R.J. Smernik
Biochar carbon stability in a clayey soil as a function of feedstock and pyrolysis temperature
Environmental Science & Technology, 46 (2012), pp. 11770-11778

52. **Stekhoven and Buehlmann, 2012**
D. Stekhoven, P. Buehlmann
MissForest – non-parametric missing value imputation for mixed-type data
Bioinformatics, 28 (2012), pp. 112-118

53. **Wang et al., 2013**
T. Wang, M. Camps-Arbestain, M. Hedley
Predicting C aromaticity of biochars based on their elemental composition
Organic Geochemistry, 62 (2013), pp. 1-6

54. **Wiedemeier et al., 2013**

D.B. Wiedemeier, M.D. Hilf, R.H. Smittenberg, S.G. Haberle, M.W.I.Schmidt
Improved assessment of pyrogenic carbon quantity and quality in environmental samples by high-performance liquid chromatography
Journal of Chromatography A, 1304 (2013), pp. 246-250

55. **Wiedemeier et al., 2015**
D.B. Wiedemeier, S. Brodowski, G.L.B. Wiesenberg
Pyrogenic molecular markers: linking PAH with BPCA analysis
Chemosphere, 119 (2015), pp. 432-437

56. **Wiesenberg et al., 2009**
G.L.B. Wiesenberg, E. Lehndorff, L. Schwark
Thermal degradation of rye and maize straw: lipid pattern changes as a function of temperature
Organic Geochemistry, 40 (2009), pp. 167-174

57. **Wiesenberg et al., 2010**
G.L.B. Wiesenberg, M. Gocke, Y. Kuzyakov
Fast incorporation of root-derived lipids and fatty acids into soil – evidence from a short term multiple pulse labelling experiment
Organic Geochemistry, 41 (2010), pp. 1049-1055

58. **Wolf et al., 2013**
M. Wolf, E. Lehndorff, G.L.B. Wiesenberg, M. Stockhausen, L. Schwark, W.Amelung
Towards reconstruction of past fire regimes from geochemical analysis of charcoal
Organic Geochemistry, 55 (2013), pp. 11-21

59. **Wood, 1988**
D.J. Wood
Characterization of charcoals by drift
Mikrochimica Acta, 2 (1988), pp. 167-169

60. **Yunker et al., 2002**
M.B. Yunker, R.W. Macdonald, R. Vingarzan, R.H. Mitchell, D. Goyette, S.Sylvestre
PAHs in the Fraser River basin: a critical appraisal of PAH ratios as indicators of PAH source and composition
Organic Geochemistry, 33 (2002), pp. 489-515